1521-0103/365/2/368–378$35.00
THE JOURNAL OF PHARMACOLOGY AND EXPERIMENTAL THERAPEUTICS

https://doi.org/10.1124/jpet.117.246652
J Pharmacol Exp Ther 365:368–378, May 2018

The Journal of PHARMACOLOGY And Experimental Therapeutics

Generation and Characterization of a Novel Small Biologic Alternative to Proprotein Convertase Subtilisin/Kexin Type 9 (PCSK9) Antibodies, DS-9001a, Albumin Binding Domain–Fused Anticalin Protein[S]

Yusuke Masuda,[1] Shinji Yamaguchi,[1] Chikako Suzuki, Takahide Aburatani, Yuki Nagano, Ryuki Miyauchi, Eiko Suzuki, Naotoshi Yamamura, Kentaro Nagatomo, Hidetoshi Ishihara, Kazuaki Okuno, Futoshi Nara, Gabriele Matschiner, Ryuji Hashimoto, Tohru Takahashi, and Tomohiro Nishizawa

End-Organ Disease Laboratories (Y.M., Y.N., T.N.), Venture Science Laboratories (S.Y.), Modality Research Laboratories (C.S., T.A., R.M., R.H., T.T.), Drug Metabolism & Pharmacokinetics Research Laboratories (E.S., N.Y.), Biologics Technology Research Laboratories (K.N., H.I., K.O.), and Biologics & Immuno-Oncology Laboratories (F.N.), Daiichi Sankyo Co., Ltd., Tokyo, Japan; and Pieris Pharmaceuticals GmbH, Freising, Germany (G.M.)

Received December 13, 2017; accepted February 15, 2018

ABSTRACT

Since it was recently reported that an antibody for proprotein convertase subtilisin/kexin type 9 (PCSK9) reduces the risk of cardiovascular events in a clinical context, PCSK9 inhibition is thought to be an attractive therapy for dyslipidemia. In the present study, we created a novel small biologic alternative to PCSK9 antibodies called DS-9001a, comprising an albumin binding domain fused to an artificial lipocalin mutein (ABD-fused Anticalin protein), which can be produced by a microbial production system. DS-9001a strongly interfered with PCSK9 binding to low-density-lipoprotein receptor (LDL-R) and PCSK9-mediated degradation of LDL-R. In cynomolgus monkeys, single DS-9001a administration significantly reduced the serum LDL-C level up to 21 days (62.4% reduction at the maximum). Moreover, DS-9001a reduced plasma non–high-density-lipoprotein cholesterol and oxidized LDL levels, and their further reductions were observed when atorvastatin and DS-9001a were administered in combination in human cholesteryl ester transfer protein/ApoB double transgenic mice. Additionally, their reductions on the combination of atorvastatin and DS-9001a were more pronounced than those on the combination of atorvastatin and anacetrapib. Besides its favorable pharmacologic profile, DS-9001a has a lower molecular weight (about 22 kDa), yielding a high stoichiometric drug concentration that might result in a smaller administration volume than that in existing antibody therapy. Since bacterial production systems are viewed as more suited to mass production at low cost, DS-9001a may provide a new therapeutic option to treat patients with dyslipidemia. In addition, considering the growing demand for antibody-like drugs, ABD-fused Anticalin proteins could represent a promising new class of small biologic molecules.

Introduction

Proprotein convertase subtilisin/kexin type 9 (PCSK9) is a member of the proteinase K secretory subtilisin-like subfamily of serine proteases and is expressed mainly in the liver, kidney, and small intestine. PCSK9 binds to the low-density-lipoprotein receptor (LDL-R) and induces its degradation. Thus, PCSK9 inhibitors that block PCSK9-mediated LDL-R degradation reduce the plasma low-density-lipoprotein cholesterol (LDL-C) level (Dadu and Ballantyne, 2014). Strong evidence for the impact of PCSK9 on circulating LDL-C level and cardiovascular events has been provided by human genetic studies. Mutations in PCSK9 can lead to changes in its activity (gain or loss of function) that correlate with elevated or decreased plasma LDL-C levels and the risk of cardiovascular events (Abifadel et al., 2009). Moreover, recently, the treatment of statin-treated patients with evolocumab, a monoclonal anti-PCSK9 antibody, reduced cardiovascular events (Sabatine et al., 2017). Therefore, PCSK9

This work was supported by Daiichi Sankyo Co., Ltd.
[1]Y.M. and S.Y. contributed equally to this work.
https://doi.org/10.1124/jpet.117.246652.
[S] This article has supplemental material available at jpet.aspetjournals.org.

ABBREVIATIONS: ABD, albumin binding domain; AUC, area under the curve; BSA, bovine serum albumin; CETP, cholesteryl ester transfer protein; DiI-LDL, 1,1′-dioctadecyl-3,3,3′,3′-tetramethyl-indocarbocyanine perchlorate; DMEM, Dulbecco's modified Eagle's medium; ELISA, enzyme-linked immunosorbent assay; HDL-C, high-density-lipoprotein cholesterol; HRP, horseradish peroxidase; HSA, human serum albumin; IACUC, Institutional Animal Care and Use Committee; k_a, association rate constant; K_D, dissociation constant; k_d, dissociation rate constant; LDL-C, low-density-lipoprotein cholesterol; LDL-R, low-density-lipoprotein receptor; ox-LDL, oxidized low-density lipoprotein; PBS, phosphate-buffered saline; PCSK9, proprotein convertase subtilisin/kexin type 9; TC, total cholesterol; TG, triglyceride; $t_{1/2}$, elimination half-life.

inhibition is a promising therapeutic strategy for dyslipidemia. Antibodies on the market for treating dyslipidemia have a complex structure and a large size, however, leading to high production costs and a relatively high administration volume of the drug. Both these issues can be solved with a PCSK9 inhibitor of a smaller molecular size.

Lipocalins are a family of proteins composed of a target-binding loop region with high plasticity and a structurally rigid β-barrel scaffold. By introducing random mutations into their loop region and selecting products using their binding affinity to target proteins, it is possible to create artificial lipocalins that potently and specifically recognize the target protein, called Anticalin proteins (Skerra, 2008). To date, we have reported tear lipocalin-derived Anticalin proteins that potently bind to VEGF-A (Gille et al., 2016) or to the extracellular domain of the c-met receptor (Olwill et al., 2013). Besides their vast repertoire of recognized ligands, Anticalin proteins can be easily produced by bacterial expression systems and exhibit robust biophysical properties. Although naked Anticalin proteins have been reported to disappear rapidly from the blood, their plasma elimination half-life ($t_{1/2}$) could be extended by connecting effector domains, such as via site-directed PEGylation (Gille et al., 2016). Considering these properties, Anticalin proteins with long $t_{1/2}$ values could be attractive pharmacologic tools for PCSK9 inhibition.

In the present study, we generated an albumin-binding domain–fused Anticalin protein (DS-9001a) that potently inhibits the binding of PCSK9 to LDL-R and has a long $t_{1/2}$ by binding to circulating albumin. We investigated its pharmacokinetic and pharmacologic profiles in rodents and cynomolgus monkeys. We also compared the combined effects of DS-9001a and atorvastatin to the combination treatment of cholesteryl ester transfer protein (CETP) inhibitor, anacetrapib, and atorvastatin, or each monotherapy alone, on plasma lipid profiles.

Materials and Methods

Animals. Male Sprague-Dawley rats and male C57BL/6J mice were purchased from Charles River Laboratories Japan, Inc. (Yokohama, Japan). Male B6.SJL-Tg(APOA-CETP)1Dsg Tg(APOB)1102-Sgy N10 mice (human CETP/ApoB double Tg mice) were purchased at 7 weeks of age from CLEA Japan, Inc. (Tokyo, Japan). Animals were acclimatized for more than 3 days. Two to three rats or five mice were housed per cage and were given rodent chow (FR-2; Funabashi Farm Co., Ltd., Funabashi, Japan) and tap water ad libitum. All experimental procedures were approved by the Institutional Animal Care and Use Committee (IACUC) of Daiichi Sankyo Co., Ltd. The experiments were performed in accordance with this committee's guidelines.

Production of Recombinant PCSK9 Protein. Human PCSK9 containing a C-terminal FLAG tag (hPCSK9-Flag) was expressed in transfected human embryonic kidney cell line HEK293F. Six hundred milliliters of transfected cells were cultivated in Dulbecco's modified Eagle's medium (DMEM)/ITS (insulin, transferrin, and selenium) containing 0.05% bovine serum albumin (BSA) for 6 days, and the supernatant containing the produced hPCSK9-Flag was collected. hPCSK9-Flag was bound to FLAG M2 resin, washed with 50 column volumes of wash buffer (10 mM Tris-HCl, pH7.4, 150 mM NaCl, 2 mM $CaCl_2$, 10% glycerol), and eluted with wash buffer containing 100 μg/ml 3× FLAG peptide. The eluted protein was further purified via gel filtration using a Superdex 200 16/60 column (GE Healthcare, Little Chalfont, UK).

For selection and screening of Anticalin proteins of interest, hPCSK9-Flag was biotinylated by incubation with a five times molar excess of EZ-Link NHS-Chromogenic Biotin reagent (Thermo Fisher Scientific, Waltham, MA) for 1 hour at room temperature. Excess biotin was removed, and the biotinylated protein was concentrated by ultrafiltration. The gain-of-function human PCSK9_D374Y mutant (Cameron et al., 2006), cynomolgus PCSK9, and mouse PCSK9 were produced and characterized in the same way.

Generation of a Library with 2×10^{10} Independent Anticalin Proteins and Phage Selection of Anticalin Proteins against PCSK9. A random library of 2×10^{10} Anticalin proteins with high diversity was generated by random mutagenesis of mature human tear lipocalin (Gille et al., 2016). For selection of PCSK9-specific Anticalin proteins, 2×10^{12} phages from this library were incubated with 200 nM biotinylated human and/or cynomolgus PCSK9. Paramagnetic beads coated with neutravidin or streptavidin were used to capture PCSK9/phage complexes, which were subsequently isolated with a magnet. Unbound phages were removed by washing the beads eight times with 1 ml of phosphate-buffered saline (PBS) supplemented with 0.1% Tween-20 (v/v) (PBS-0.1%T). Bound phages were eluted by incubation first with triethylamine and then with 0.1 M glycine pH 2.2. Four consecutive rounds of selection were performed.

The mutagenized central cassette of the plasmid preparation obtained after phage display selection was isolated by digestion of the DNA with BstX1 and subsequent purification via agarose gel electrophoresis using standard methods. The DNA was inserted into the similarly cut vector pTlc10, which allows bacterial production of the Anticalin proteins under the control of a tetracycline promoter. $CaCl_2$-competent TG1-F' cells were transformed with the ligation mixture and plated on LB/Amp plates. Individual colonies were used to inoculate 2xYT/Amp medium and grown overnight (14–18 hours) to stationary phase. Subsequently, 50 μl of 2xYT/Amp was inoculated from the stationary-phase cultures and incubated for 3 hours at 37°C and then shifted to 22°C until an OD_{595} of 0.6–0.8 was reached. Anticalin protein production was induced by the addition of 10 μl of 2xYT/Amp supplemented with 1.2 μg/ml anhydrotetracycline. Cultures were incubated at 22°C until the next day. After the addition of 40 μl of 5% (w/v) BSA in PBS-0.1%T and incubation for 1 hour at 25°C, cultures were ready for use in screening assays.

For the selection of Anticalin proteins, enzyme-linked immunosorbent assay (ELISA) assay was performed. Specifically, human and cynomolgus PCSK9 (1 μg/ml in PBS-0.1%T), which all carried a FLAG-tag, were captured on microplates using an anti-FLAG-tag antibody (Sigma-Aldrich, St. Louis, MO), which had been coated on the plates the day before at a final concentration of 5 μg/ml in PBS. The anti-Flag-tag antibody alone served as a negative control. Subsequently, 20 μl of BSA-blocked cultures were added and incubated for 1 hour at 25°C. Bound Anticalin proteins were detected with a 1:10,000 dilution of anti-T7 antibody conjugated with horseradish peroxidase [horseradish peroxidase (HRP), Merck KgaA, Darmstadt, Germany) in PBS-0.1%T. For quantification, 20 μl of QuantaBlu fluorogenic peroxidase substrate was added and measured at an excitation wavelength of 320 nm and an emission wavelength of 430 nm.

Generation of a Biased Maturation Library for Optimization of PCSK9-Specific Anticalin Proteins. For optimization of PCSK9-specific Anticalin proteins, additional libraries were generated based on initial hit clones (or parental Anticalin proteins). The libraries were generated in a manner that led to partial randomization of selected positions only by recursive polymerase chain reaction. Subsequently, the generated Anticalin proteins were cloned with high efficiency into a phagemid vector essentially as described previously (Kim et al., 2009). The library size ranged from 7×10^9 to 11×10^9 mutants. The libraries were used in subsequent phage panning (Supplemental Methods).

Identification of PCSK9-Specific Anticalin Proteins by Screening. Selected Anticalin proteins from optimized Anticalin proteins were produced by *Escherichia. coli* and further selected in an ELISA assay as described herein using the hPCSK9_D374Y

mutant to capture human and cynomolgus PCSK9. After the addition of 40 μl of 5% (w/v) BSA in PBS-0.1%T and incubation for 1 hour at 25°C, cultures were ready for use in screening assays.

For affinity ranking of Anticalin proteins, anti-Strep-tag antibody (IBA Lifesciences, Goettingen, Germany) in PBS was coated on microplates, and 20 μl of BSA-blocked cultures were added, which allowed specific capture of Anticalin proteins on the plate. Different concentrations (0.5–5 nM) of biotinylated PCSK9 proteins were added, and specifically bound PCSK9 proteins were detected with extravidin-HRP (Sigma-Aldrich) after extensive washing. For quantification, 20 μl of QuantaBlu was added and measured at an excitation wavelength of 320 nm and an emission wavelength of 430 nm.

The selection of competitive Anticalin proteins that can block the interaction of PCSK9 with LDL-R was performed by coating anti-FLAG-tag (5 μg/ml in PBS) on microplates and subsequently capturing hPCSK9-D374Y mutant (1 μg/ml in PBS-0.1%T). BSA-blocked cultures were adjusted to 30 nM recombinant human LDL-R containing a C-terminal His tag and added for 72 hours to plates with captured hPCSK9-D374Y mutant. This allowed equilibration of the system and the reliable selection of competitive Anticalin proteins. Bound receptor was detected with an HRP-conjugated anti-His-tag antibody (1 μg/ml in PBS-0.1%T; Abcam, Cambridge, UK). For quantification, 20 μl of QuantaBlu fluorogenic peroxidase substrate was added and measured at an excitation wavelength of 320 nm and an emission wavelength of 430 nm.

Expression and Purification of PCSK9-Specific Anticalin Protein and DS-9001a. From the biased maturation library screening, a PCSK9-specific Anticalin protein was obtained. This Anticalin protein was genetically fused with a deimmunized albumin binding domain (ABD) variant (Zurdo et al., 2015), and the fusion molecule was denoted DS-9001a (refer to seq. ID no. 83; Matschiner et al., 2014). DNA encoding DS-9001a or DS-9001a without ABD was inserted into a similarly cut vector, which allowed bacterial production under the control of a T5 promoter or a T7A3 promoter and expressed in *E. coli*. The proteins were purified from cell lysates by a combination of column chromatography methods using an anion exchange column, phenyl Sepharose column, and gel filtration column. The purified proteins were finally solubilized in PBS. DS-9001a was also produced using a Gram-positive *Corynebacterium glutamicum* expression system (CORYNEX) of Ajinomoto Co., Inc. (Tokyo, Japan). The concentrations of undiluted purified DS-9001a used for the pharmacodynamic studies were 99.6–101.4 mg/ml (approximately 4.5–4.6 mM). Since these concentrations were too high to administer the intended amount of DS-9001a in rodents and monkeys accurately owing to their small body weights, we diluted DS-9001a with control buffer and used this in the present study.

Evaluation of DS-9001a's Pharmacokinetic Profile in Rats. DS-9001a or DS-9001a without ABD was intravenously injected into male Sprague-Dawley rats (9 weeks old) at 10 or 7.6 mg/kg, respectively, which are equivalent to 0.45 μmol/kg ($n = 3$). Administration was conducted at 2.0 ml/kg. Blood was collected from the tail vein at 0.5, 1, 2, 4, 6, 8, 10, 24, 48, and 72 hours after injection. Plasma was obtained by centrifugation (12,000 rpm, 5 minutes, 4°C). Detailed methods to evaluate the pharmacokinetic profile of DS-9001a and DS-9001a without ABD are described in Supplemental Method.

Measurement of Binding Affinity of DS-9001a and DS-9001a without ABD to Human PCSK9 and Human Serum Albumin. To measure the binding affinity of DS-9001a and DS-9001a without ABD to biotinylated PCSK9, a surface plasmon resonance-based assay was employed using a Biacore T200 instrument (GE Healthcare) (Supplemental Method). The association rate constants (k_a), dissociation rate constants (k_d), and resulting dissociation constants (K_D) were calculated using a 1:1 Langmuir binding model.

PCSK9 and LDL-R Binding Inhibition Assay. For this assay, biotin-labeled human PCSK9 (biotin-hPCSK9) was prepared as described to follow. Recombinant human PCSK9 protein (2.1 mg/ml; Thermo Fisher Scientific) was biotinylated by incubating with 10 mM EZ-Link Sulfo-NHS-LC-LC-Biotin (Thermo Fisher Scientific) for 85 minutes at room temperature. For purification, we used a Zeba Spin Desalting Column (Thermo Fisher Scientific) pre-equilibrated in elution buffer (20 mM HEPES, pH 7.4, 2 mM $CaCl_2$, 150 mM NaCl, 10% glycerol). The labeling reaction mixture described herein was applied to the column followed by eluting with 100 μl of elution buffer by centrifugation at 1000*g* for 2 minutes at 4°C to collect purified biotin-hPCSK9.

The 2 μg/ml anti-LDL-R solution (R&D Systems, Minneapolis, MN) was added to a 96-well plate at 100 μl/well and incubated overnight at 4°C to allow adhesion of the antibody to the plate. The next day, this plate was washed three times with Dulbecco's PBS (DPBS), and the wells were incubated with DPBS containing 1% skim milk (Becton Dickinson and Company, Franklin Lakes, NJ) at room temperature for 1 hour. After the plate had been washed three times with DPBS containing 0.05% Tween 20 (DPBS-0.05%T), the reaction mixtures that contained 3 mg/ml biotin-hPCSK9 and various concentrations of DS-9001a were added to the plate at 50 μl/well ($n = 3$). Then, 0.4 μg/ml recombinant human LDL-R (R&D Systems) was added to the plate at 50 μl/well. As positive and negative controls, DS-9001a-deficient and LDL-R-deficient wells were prepared, respectively. After the plate had been incubated at room temperature for 2 hours, the wells were washed three times with DPBS-0.05%T. Pierce High Sensitivity Streptavidin-HRP (Thermo Fisher Scientific) diluted 10,000-fold in DPBS-0.05%T containing 1% BSA was added to the plate at 100 μl/well and then incubated at room temperature for 1 hour.

The luminescent signal was measured using BM Chemiluminescence ELISA substrate (POD) (Roche Diagnostics, Tokyo, Japan). After three washes with DPBS-0.05%T, POD working solution was then added to each well at 100 μl/well. The plate was incubated at room temperature for 5 minutes in the dark, and luminescent signals in each plate were measured using a multimode microplate reader (Molecular Devices, LLC, Sunnyvale, CA). The relative binding activity was calculated for each well using the following formula: Relative binding activity (%) = [(luminescent signal in each well) − (luminescent signal in negative control wells)]/[(luminescent signal in positive control wells) − (luminescent signal in negative control wells)] × 100. In the binding inhibition assay in the presence of albumin, the reaction mixture contained 17 mg/ml human albumin (Sigma-Aldrich).

Cell-Based Inhibition of PCSK9-Mediated LDL-R Degradation Assay. HepG2 cells were seeded onto a 96-well plate and cultured with DMEM containing 10% fetal bovine serum and 1% penicillin-streptomycin (Thermo Fisher Scientific) in a CO_2 incubator (37°C with 5% CO_2) overnight. The next day, the medium was changed to DMEM containing 5% lipoprotein-deficient bovine calf serum (LPDS; Biomedical Technologies, Madrid, Spain) and 1% penicillin-streptomycin (LPDS medium), and the cells were cultured in a CO_2 incubator overnight. The next day, the medium was removed, and LPDS medium containing various concentrations of DS-9001a was added to the cells ($n = 3$). Then, LPDS medium containing 12 μg/ml of human PCSK9 was added to the cells at 25 μl/well. As positive and negative controls, DS-9001a plus PCSK9-deficient or PCSK9-deficient wells were prepared, respectively. After incubation for 6 hours in a CO_2 incubator, the medium was removed, and the cells were fixed with Mildform10N at room temperature for 20 minutes. The cells were then washed five times with PBS and incubated with PBS-0.1% NaN_3-1% H_2O_2 solution at room temperature for 20 minutes with gentle shaking. After the cells had been washed five times with PBS, they were incubated with PBS containing 3% BSA at room temperature for 90 minutes. Anti-LDL-R primary antibody (Progen Biotechnik, Heidelberg, Germany) diluted 600-fold in PBS containing 3% BSA was added to the cells and incubated at room temperature for 60 minutes. Then, the cells were washed five times with PBS and incubated with anti-rabbit IgG, HRP-Linked F(ab′)2 Fragment (GE Healthcare) diluted 2000-fold in PBS containing 3% BSA at room temperature for 60 minutes. The luminescent signal was measured using POD (Roche Diagnostics). The cells were washed five times with PBS, after which POD working solution was added to each well at 75 μl/well.

The plate was incubated at room temperature for 5 minutes in the dark, and luminescent signals were measured using a multimode microplate reader (Molecular Devices, LLC) and calculated using the following formula: relative activity (%) = [(luminescent signal in each well) – (luminescent signal in negative control wells)]/[(luminescent signal in positive control wells) − (luminescent signal in negative control wells)] × 100. The amount of DS-9001a required for 50% inhibition of PCSK9 function (IC_{50}) was determined by using a sigmoid Emax model, and the analyses were performed using SAS System Release 9.2 (SAS Institute Inc., Cary, NC).

Inhibition of PCSK9-Mediated LDL-R Degradation in Mice. Vehicle, 0.3, or 3.0 mg/5.0 ml/kg DS-9001a was administered intravenously into mice. Thirty minutes after DS-9001a administration, 0.8 mg/kg mouse PCSK9 was administered intravenously. Liver was obtained 60 minutes after PCSK9 administration. Liver samples were lysed with RIPA buffer (Merck Millipore, Billerica, MA) with protease inhibitor (Nacalai Tesque, Kyoto, Japan) and centrifuged at 15,000 rpm and 4°C for 10 minutes. Supernatant was obtained, and protein amounts were measured by a Pierce BCA Protein assay kit. An equal amount of protein was used for Western blot analysis. LDL-R and β-actin were detected by anti-LDL-R antibody (R&D Systems) and anti-β-actin antibody (Cell Signaling Technology, Danvers, MA), respectively.

DiI-Labeled LDL Clearance Assay. Approximately 24 hours before the administration of lipoprotein labeled with 1,1′-dioctadecyl-3,3,3′,3′-tetramethyl-indocarbocyanine perchlorate (DiI-labeled LDL, DiI-LDL; Biomedical Technologies), 0.3 or 3.0 mg/5.0 ml/kg DS-9001a or vehicle was administered to mice intravenously. The next day, 200 μg/ml DiI-LDL was administered, and blood was collected 2 minutes, 0.5, 1, 2, 4, and 6 hours later. Plasma was obtained by centrifugation, and the plasma DiI-LDL level was determined based on fluorescence intensity (excitation wavelength: 520 nm, measurement wavelength: 590 nm). The area under the curve (AUC) of the plasma DiI-LDL level (from 2 minutes to 6 hours after DiI-LDL injection) was calculated using the trapezoidal rule.

Atorvastatin Combination Study. Human CETP/ApoB double Tg mice were treated with DS-9001a, anacetrapib, and atorvastatin, or a combination from among these drugs. The duration of the study was 8 days. Atorvastatin was administered by mixing with food (FR-2 powder chow diet containing 0.08% atorvastatin). Anacetrapib was administered orally once daily at 10 mg/kg from the initiation of the study (day 1) to day 7. DS-9001a was administered intravenously at 30 mg/kg on days 1, 4, and 7. The dosing volume of DS-9001a was calculated to be 5.0 ml/kg based on the body weight. Blood was collected on day 8, and plasma triglyceride (TG) and total cholesterol (TC) were measured using triglyceride E-test Wako (Wako Pure Chemical Industries, Ltd., Osaka, Japan) and cholesterol E-test Wako (Wako Pure Chemical Industries, Ltd.), respectively. The ratio of high-density lipoprotein (HDL) and non-HDL was determined using an HPLC system (Tosoh Corporation, Tokyo, Japan), as described previously (Shimizugawa et al., 2002), and each cholesterol level was calculated by dividing plasma TC levels according to the ratio. Plasma oxidized LDL (ox-LDL) level was measured using an oxidized LDL ELISA kit (Mercodia AB, Uppsala, Sweden). Plasma PCSK9 level was measured using Mouse Proprotein Convertase 9/PCSK9 Quantikine ELISA Kit (R&D Systems).

Studies in Monkeys. Male cynomolgus monkeys (2.8–6.0 kg) were maintained at Shin Nippon Biomedical Laboratories, Ltd., Drug Safety Research Laboratories (Kagoshima, Japan) under standard environmental conditions in individual cages. Solid food (HF Primate J 12G 5K9J; Purina Mills, LLC, Gray Summit, MO) was provided to each animal once daily and was available ad libitum from an automatic supply system. The study was approved by the IACUC (approval no. IACUC315-218) and was performed in accordance with the animal welfare bylaws of SNBL DSR, which is accredited by AAALAC International. Here, 0.3, 1, or 3 mg/kg DS-9001a or vehicle was administered intravenously to monkeys. The dosing volume was calculated to be 1 ml/kg based on body weight. The endotoxin level in each dose was below 0.18 EU/kg, and this value fell below the acceptable threshold for use in animals (Malyala and Singh, 2008). Serum LDL-C and high-density-lipoprotein cholesterol (HDL-C) levels were measured by an automatic analyzer (JEOL Ltd., Tokyo, Japan).

Results

Generation and Characterization of PCSK9-Specific ABD-Fused Anticalin Protein, DS-9001a. Anticalin proteins targeting PCSK9 were generated by using tear lipocalin-based phage display Anticalin libraries in selections against human PCSK9, the gain-of-function human PCSK9_D374Y mutant, and cynomolgus PCSK9. The affinity of selected Anticalin proteins to PCSK9 was ranked, and through evaluation of the ability to block the interaction of PCSK9 and LDL-R, we identified a PCSK9-specific Anticalin protein. Since the Anticalin protein itself was expected to be rapidly eliminated from the body, ABD was fused to its C-terminus to prolong the $t_{1/2}$ (Fig. 1A).

Binding kinetics of DS-9001a and DS-9001a without ABD were measured using surface plasmon resonance (Biacore). The determined k_a, k_d, and K_D are summarized in Table 1. Both DS-9001a and DS-9001a without ABD bind to human PCSK9, with K_D on the order of nanomoles, suggesting that 1) the Anticalin protein moiety of DS-9001a potently interacts with PCSK9, and 2) fusion with ABD does not influence its

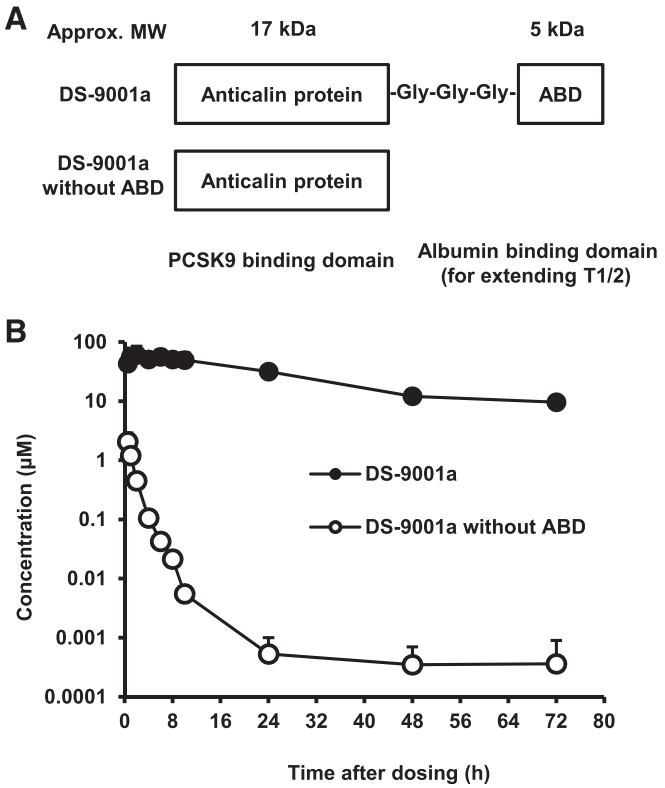

Fig. 1. Pharmacokinetics of DS-9001a and DS-9001a ABD. (A) Schematic illustration of DS-9001a structure. The Anticalin protein was genetically fused with ABD)through a Gly-Gly-Gly linker to extend the $t_{1/2}$. The approximate molecular weight (MW) is indicated. (B) DS-9001a or DS-9001a without ABD was intravenously injected into male Sprague-Dawley (SD) rats (9 weeks old) at 10 or 7.6 mg/kg, respectively, which are equivalent to 0.45 μmol/kg. Blood was collected from the tail vein at 0.5, 1, 2, 4, 6, 8, 10, 24, 48, and 72 hours after injection. Plasma DS-9001a and DS-9001a without ABD were measured. The results are presented as mean + S.E. (n = 3).

affinity to PCSK9. The binding of DS-9001a to HSA was confirmed in this assay (K_D = 0.019 nM).

To confirm the effect of ABD on extending plasma $t_{1/2}$, pharmacokinetic profiles after single dosing of DS-9001a and DS-9001a without ABD to rats were examined. Plasma concentration-time profiles after intravenous administration of 10 mg/kg DS-9001a and 7.6 mg/kg DS-9001a without ABD, which corresponded to equal amounts of protein, are shown in Fig. 1B. Plasma $t_{1/2}$ of DS-9001a was 24.3 ± 3.1 hours, whereas that of DS-9001a without ABD was 0.992 ± 0.095 hours. This suggests that ABD dramatically extends the $t_{1/2}$ of DS-9001a by tightly binding to circulating albumin in vivo.

DS-9001a Inhibits PCSK9-Dependent LDL-R Degradation. We examined the effects of DS-9001a on the binding between human PCSK9 and LDL-R in an in vitro cell-free assay. After the addition of a mixture of DS-9001a and human PCSK9 to an LDL-R–coated plate, the immobilized PCSK9 level was measured. As shown in Fig. 2A, DS-9001a reduced the immobilized PCSK9 level in a dose-dependent manner, suggesting that DS-9001a inhibits the PCSK9 binding to LDL-R. Since DS-9001a binds to both PCSK9 and albumin, we next examined whether this inhibitory effect of DS-9001a was interfered with by the presence of albumin. As shown in Fig. 2B, we confirmed that the inhibitory activity of DS-9001a was maintained, even in the presence of albumin. This inhibitory effect was also observed in mouse, rat, and monkey PCSK9 (Supplemental Fig. 1). To verify that DS-9001a disturbs the PCSK9-mediated LDL-R degradation, as previously demonstrated by anti-PCSK9 antibody (Liang et al., 2012), HepG2 cells were incubated with DS-9001a and PCSK9, and the cell surface LDL-R level was determined using anti-LDL-R antibody. The treatment of PCSK9 reduced cell-surface LDL-R expression, and DS-9001a treatment reversed it, with an IC_{50} value of 6.7 nM (Fig. 2C), indicating that DS-9001a potently inhibits PCSK9-mediated LDL-R degradation. To evaluate further the PCSK9 inhibitory effect of DS-9001a in vivo, DS-9001a and PCSK9 were injected into mice, and the hepatic LDL-R level was determined. As shown in Fig. 2D, the administration of DS-9001a before PCSK9 injection rescued PCSK9-mediated LDL-R reduction. All these findings together suggest that DS-9001a is a potent and functional PCSK9 inhibitor both in vitro and in vivo.

DS-9001a Enhances LDL-C Clearance in Mice. Next, to determine the effect of DS-9001a on the metabolism of LDL-C in vivo, we injected DiI-LDL into C57BL/6J mice approximately 24 hours after the administration of DS-9001a and determined the transition of plasma DiI-LDL concentrations (Fig. 3A). A single intravenous administration of DS-9001a at dosages of 0.3 and 3.0 mg/kg before DiI-LDL injection showed statistically significant lowering of the AUC of the plasma DiI-LDL level (from 2 minutes to 6 hours after DiI-LDL injection) in a dose-dependent manner (Fig. 3B). This finding suggests that DS-9001a treatment enhances LDL-C clearance in vivo.

DS-9001a Reduces LDL-C in Cynomolgus Monkeys. To examine further the pharmacologic profile of DS-9001a in lipid metabolism, DS-9001a was administered intravenously at dose levels of 0 (control), 0.3, 1, and 3 mg/kg to healthy cynomolgus monkeys. Single DS-9001a administration significantly decreased serum LDL-C from 24 hours after dosing, which then returned to the same level as the predosing value within 240, 504, and 672 hours from dosing at 0.3, 1, and 3 mg/kg, respectively (Fig. 4A). The duration of the LDL-C suppressive effect was prolonged in a dose-dependent manner. The PCSK9 level was reported to reach the maximum value at 10 days after single intravenous injection of 10 mg/kg 1B20, an anti-PCSK9 antibody, or 5 mg/kg BMS-962476, a small biologic PCSK9 inhibitor, in monkey (Zhang et al., 2012; Mitchell et al., 2014). In the present study, the serum DS-9001a level at 10 days after the administration of 3 mg/kg DS-9001a was approximately 1 μM, which was considerably higher than the reported baseline (5 nM) and maximum (15–27 nM) monkey PCSK9 levels. The terminal $t_{1/2}$ of DS-9001a in the 3-mg/kg injection group was 128 ± 90 hours (Supplemental Fig. 2). There were no differences in serum HDL-C between the DS-9001a and control groups (Fig. 4B). Subcutaneous injection is performed for the current anti-PCSK9 antibody therapies. Plasma $t_{1/2}$ value was 116 ± 49 hours when 3 mg/kg DS-9001a was administered to cynomolgus monkeys by subcutaneous injection, which was a similar value to that in intravenous injection. The absolute bioavailability was approximately 90% (data not shown). These results suggest that DS-9001a has a potent ability to elicit a sustained LDL-C reduction via beneficial binding to albumin in vivo.

Synergistic Effect of DS-9001a with Atorvastatin on the Reduction of Plasma Non-HDL-C and Ox-LDL Levels. Since statin treatment is reported to increase both LDL-R and PCSK9 levels (Dubuc et al., 2004), it has often been proposed in the literature that there is a synergistic effect between statin and PCSK9 inhibitor (Rashid et al., 2005; Chan et al., 2009; Liang et al., 2012). In line with this theory, DS-9001a administration to mice showed an increase in hepatic LDL-R, which was further increased in combination with atorvastatin (Fig. 5A).

Since CETP inhibitor increases HDL-C and reduces LDL-C levels, this inhibitor is thought to be another potential drug candidate for dyslipidemia (Bochem et al., 2013). Indeed, many studies reported that PCSK9 and CETP inhibitors were efficacious for the treatment of dyslipidemia. Nevertheless, no reports have reported comparison of the effects of these two classes of compounds and each combination with

TABLE 1

Measurement of binding affinity of DS-9001a and DS-9001a without ABD to human PCSK9 and HSA

The binding affinities of DS-9001a and DS-9001a without ABD to biotinylated PCSK9 and HSA were measured by a surface plasmon resonance (SPR)-based assay. The association rate constants (k_a) and dissociation rate constants (k_d) were determined and the dissociation constants (K_D) were calculated based on them.

Molecule	Anti-PCSK9			Anti-HSA		
	k_a (1/Ms)	k_d (1/s)	K_D (M)	k_a (1/Ms)	k_d (1/s)	K_D (M)
DS-9001a	7.1E+05	2.7E−04	3.8E−10	2.2E+06	4.2E−05	1.9E−11
DS-9001a without ABD	1.1E+05	2.9E−04	2.6E−10			

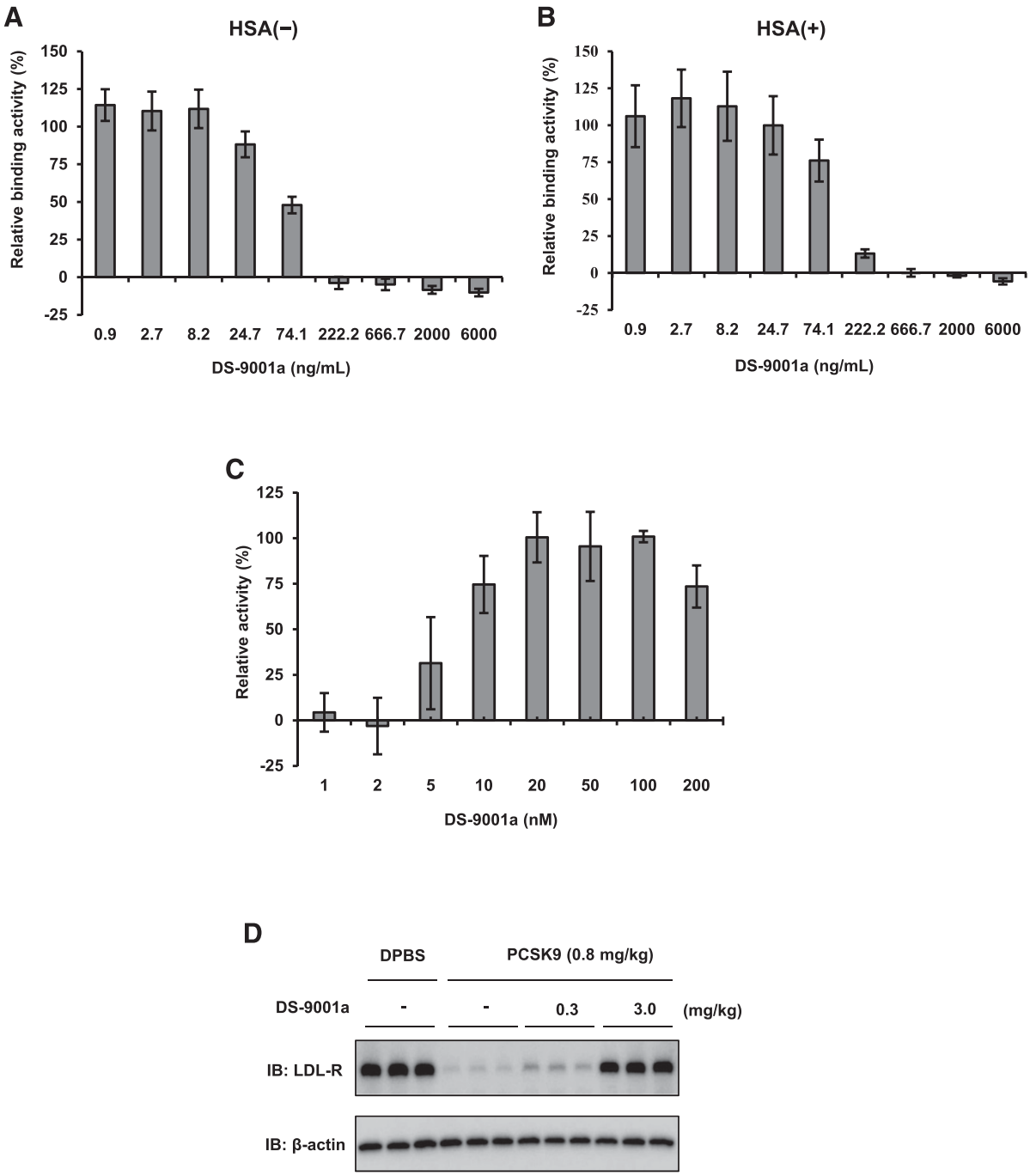

Fig. 2. DS-9001a prevents PCSK9-dependent LDL-R degradation. Biotin-labeled human PCSK9 and DS-9001a were added to an anti-LDL-R antibody-coated plate in the (A) absence or (B) presence of human serum albumin (HSA). Then, human LDL-R was added to the plate, and the plate was incubated for 2 hours. The level of PCSK9 captured by LDL-R was detected with streptavidin-HRP. As positive and negative controls, DS-9001a-deficient and LDL-R-deficient wells were prepared, respectively. The relative binding activity (%) was calculated using the following equation: Relative binding activity = [(luminescent signal in each well) − (luminescent signal in negative control wells)]/[(luminescent signal in positive control wells) − (luminescent signal in negative control wells)] × 100. The results are presented as mean ± S.E. (n = 3). (C) After HepG2 cells had been treated with DS-9001a, human PCSK9 protein was added to the cells and incubated for 6 hours. The level of cell-surface LDL-R was detected with anti-LDL-R antibody. As positive and negative controls, DS-9001a and PCSK9-deficient or PCSK9-deficient wells were prepared, respectively. The relative activity (%) was calculated using the following equation: Relative binding activity = [(luminescent signal in each well) − (luminescent signal in negative control wells)]/[(luminescent signal in positive control wells) − (luminescent signal in negative control wells)] × 100. The results are presented as mean ± S.E. (n = 3). (D) Vehicle, 0.3, or 3 mg/kg DS-9001a was intravenously administered into C57BL/6J mice. Thirty minutes after DS-9001a administration, 0.8 mg/kg mouse PCSK9 was administered intravenously. Liver was obtained 60 minutes after PCSK9 administration, and lysates of liver samples were separated by SDS-PAGE and probed with anti-LDL-R antibody (n = 3).

standard therapy, namely, statin treatment, on plasma lipids. Therefore, we examined the effects of a CETP inhibitor, anacetrapib, and DS-9001a on circulating lipid profiles, as well as those of each of them in combination with atorvastatin. Human CETP/ApoB double Tg mice were treated with DS-9001a, anacetrapib, and atorvastatin or a combination from among these drugs, for a week, after which plasma lipid profiles were analyzed. As expected, atorvastatin monotherapy increased the plasma PCSK9

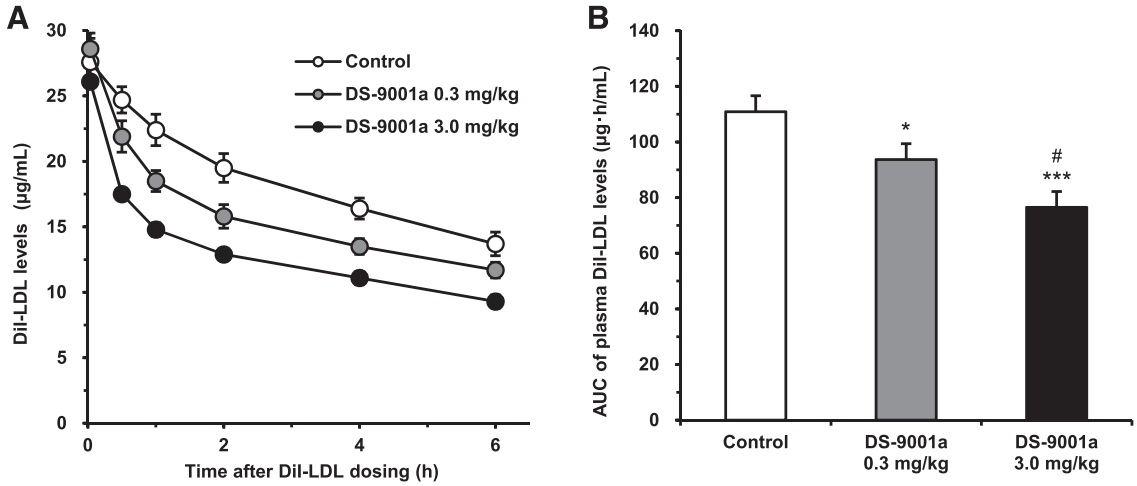

Fig. 3. DS-9001a administration enhances LDL-C clearance in C57BL/6J mice. (A) Vehicle, 0.3, or 3 mg/kg DS-9001a was intravenously administered into C57BL/6J mice. Approximately 24 hours after administration, low-density lipoprotein labeled with 1,1′-dioctadecyl-3,3,3′,3′-tetramethylindocarbocyanine perchlorate (DiI-LDL) was injected into all mice. The plasma concentrations of DiI-LDL 2 minutes, 0.5, 1, 2, 4, and 6 hours after DiI-LDL administration were measured. The results are presented as mean ± S.E. (n = 6). (B) The area under the curve (AUC) of the plasma DiI-LDL level after DiI-LDL administration (2 minutes to 6 hours). The results are presented as mean + S.E. (n = 6). $^{*}P < 0.05$; $^{***}P < 0.001$, statistically significant compared with the control group, $^{\#}P < 0.05$, statistically significant compared with the group with DS-9001a at 0.3 mg/kg (Tukey's test).

level (Fig. 5B). The increase in PCSK9 level on the coadministration of atorvastatin and anacetrapib was similar to of atorvastatin monotherapy. The plasma PCSK9 level in DS-9001a–treated mice was considerably increased compared with that in control mice, and a further increase was shown in mice with the coadministration of atorvastatin. The increase in plasma PCSK9 was also observed for other PCSK9 inhibitors, such as anti-PCSK9 antibody (Zhang et al., 2012) or BMS-962476 (Mitchell et al., 2014). This phenomenon was interpreted to be due to the delayed clearance of PCSK9 through LDL-R endocytosis. Previously, anacetrapib was reported to reduce plasma PCSK9 level (Roddy et al., 2014; Millar et al., 2015; van der Tuin et al., 2015), but we did not observe a difference of this kind in anacetrapib treatment compared with vehicle treatment. The reason for this difference is unclear. Van der Tuin et al. (2015) observed PCSK9 reduction in mice, and they administered 30 mg/kg of anacetrapib for 3 to 4 weeks, but we applied it at 10 mg/kg for a week. Thus, the lower dose of anacetrapib or the relatively short period of administration in our study may have contributed to this difference.

Statin treatment is reported to inhibit very-low-density-lipoprotein cholesterol production and thereby reduce plasma TG level (Ginsberg, 1998). Consistent with this, we identified a reduction in plasma TG in atorvastatin-treated mice. This TG reduction was not enhanced in combination treatment with either anacetrapib or DS-9001a (Fig. 5C). Atorvastatin and DS-9001a monotherapies decreased the plasma TC level significantly, and notably, coadministration of atorvastatin and DS-9001a showed a further reduction compared with their respective monotherapies (Fig. 5D).

As shown in Fig. 5E, atorvastatin and DS-9001a monotherapies revealed significant reductions in plasma non-HDL-C level compared with that on vehicle administration. Anacetrapib monotherapy also exhibited a trend of non-HDL-C reduction, although this was not statistically significant. The combination treatments of DS-9001a or anacetrapib with atorvastatin further reduced the non-HDL-C level compared with their respective monotherapies. Moreover, the extent of reduction on the combination of DS-9001a and atorvastatin was greater than that on the combination of

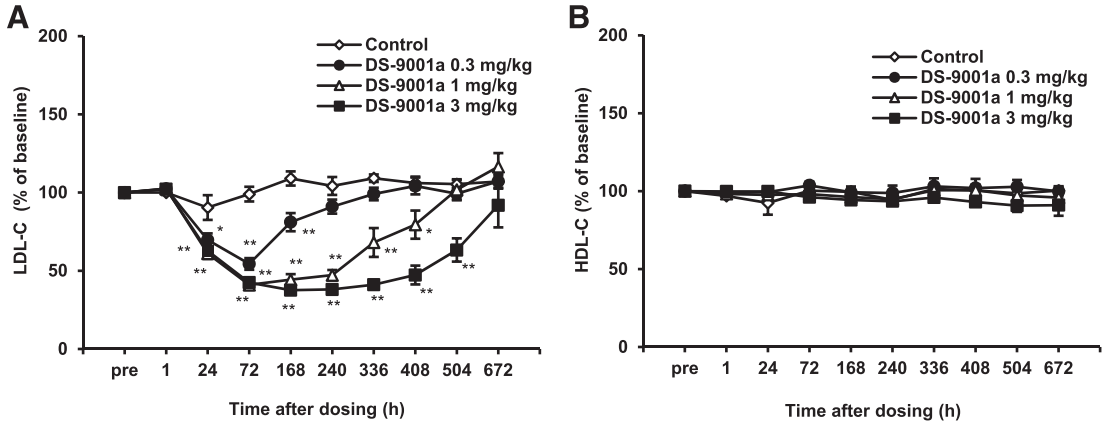

Fig. 4. Single DS-9001a administration reduces LDL-C in cynomolgus monkeys. Vehicle, 0.3, 1.0, or 3.0 mg/kg DS-9001a was intravenously administered into cynomolgus monkeys, and the blood was collected at specific time points. Serum (A) LDL-C and (B) HDL-C levels were measured. The data were calculated as the percent of change from baseline and are presented as mean ± S.E. (n = 6). $^{*}P < 0.05$; $^{**}P < 0.01$, statistically significant compared with the control group (Dunnett's test).

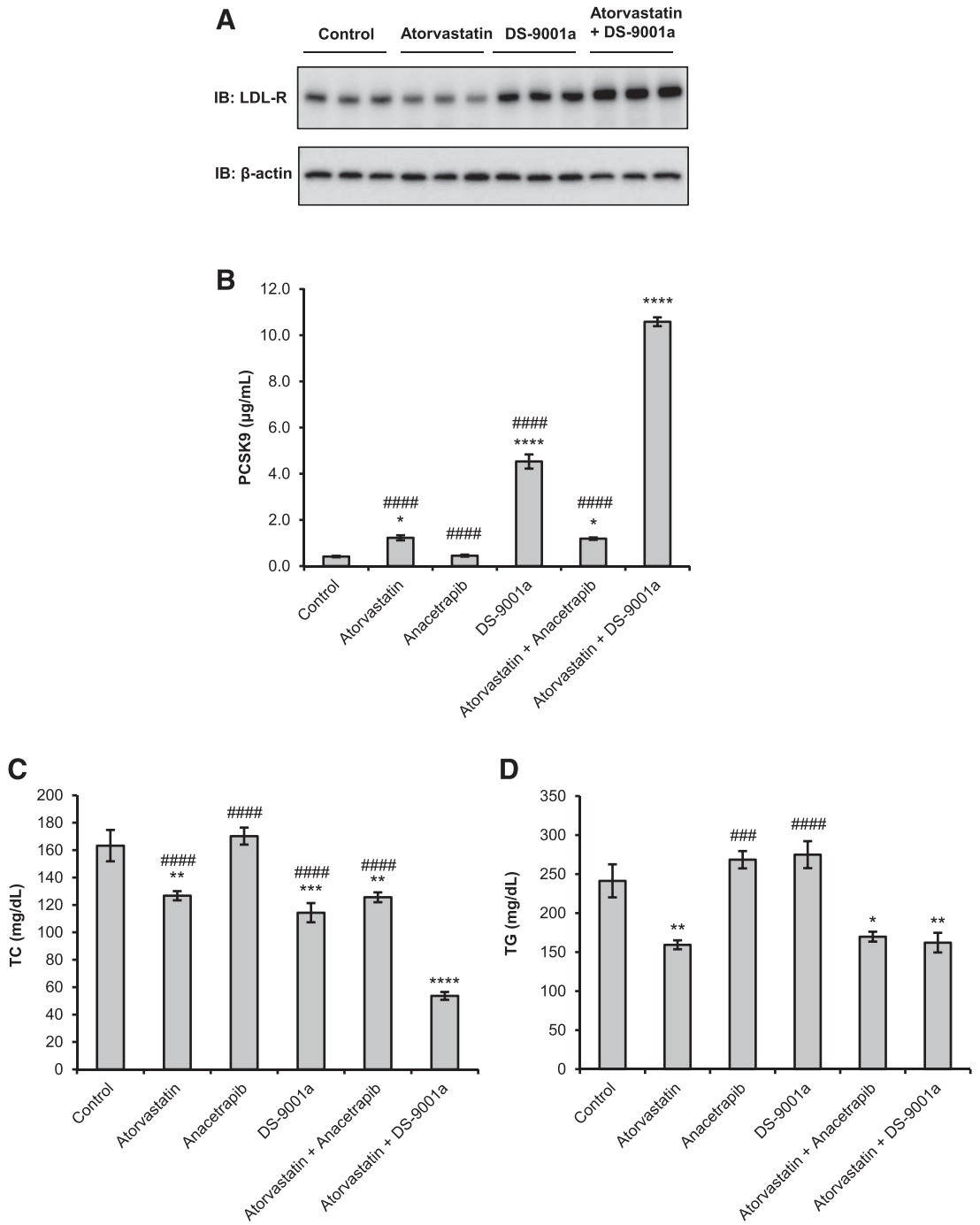

Fig. 5. Combined effects of DS-9001a with atorvastatin on plasma lipids in human CETP/ApoB double Tg mice. (A) C57BL/6J mice were treated with atorvastatin by mixing it with food (FR-2 powder chow diet containing 0.08% atorvastatin) for 5 days. Vehicle or 30 mg/kg DS-9001a was intravenously injected on day 3, liver was obtained about 48 hours after PCSK9 administration, and lysates of liver samples were separated by SDS-PAGE and probed with anti-LDL-R antibody ($n = 3$). (B–G) Male B6.SJL-Tg(APOA-CETP)1Dsg Tg(APOB)1102Sgy N10 mice (human CETP/ApoB double Tg mice) were treated for a week with DS-9001a, anacetrapib, and atorvastatin, or a combination from among these drugs. Atorvastatin was administered by mixing with food (FR-2 powder chow diet containing 0.08% atorvastatin). Anacetrapib was administered orally once daily at 10 mg/kg from the initiation of the study (day 1) to day 7. DS-9001a was administered intravenously at 30 mg/kg on days 1, 4, and 7. Blood was collected on day 8 and plasma concentrations of (B) PCSK9, (C) triglycerides (TG), (D) total cholesterol (TC), (E) non–high-density-lipoprotein cholesterol (non-HDL-C), (F) high-density-lipoprotein cholesterol (HDL-C), and (G) oxidized low-density-lipoprotein cholesterol (ox-LDL) were measured ($n = 5$). The results are presented as mean ± S.E., $n = 5$. $^{*}P < 0.05$; $^{**}P < 0.01$; $^{***}P < 0.001$; $^{****}P < 0.0001$, statistically significant compared with the control group (Tukey's test). $^{\#}P < 0.05$; $^{\#\#}P < 0.01$; $^{\#\#\#}P < 0.001$; $^{\#\#\#\#}P < 0.0001$, statistically significant compared with the atorvastatin + DS-9001a group (Tukey's test).

anacetrapib and atorvastatin, possibly owing to the synergistic effect between statin and PCSK9 inhibitor, as described already. Regarding HDL-C (Fig. 5F), anacetrapib monotherapy increased the plasma HDL-C level significantly, as expected, whereas the treatment combining anacetrapib with atorvastatin did not show an additive increase. Atorvastatin and DS-9001a monotherapies did not change the HDL-C level significantly, whereas a significant reduction compared

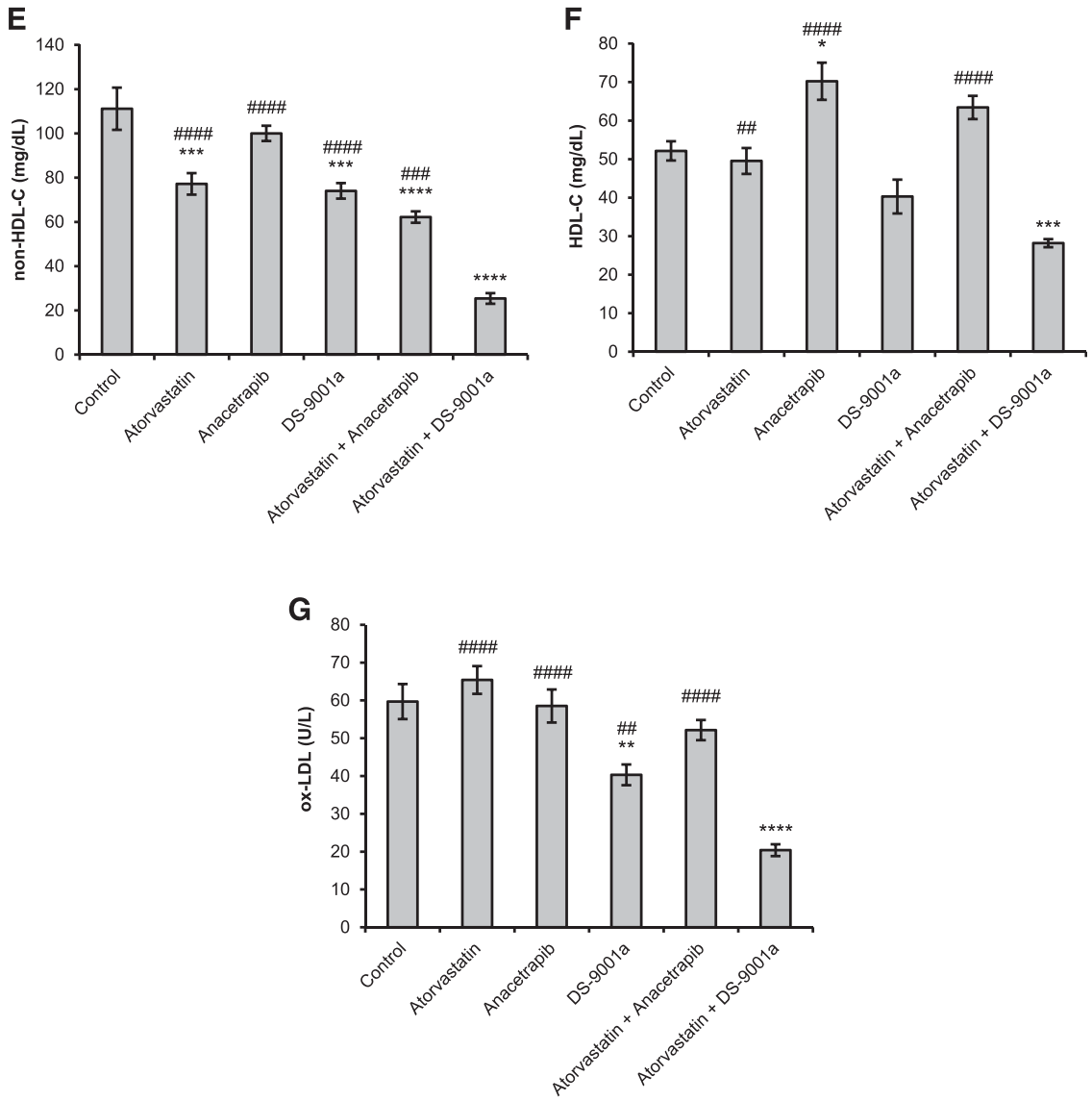

Fig. 5. Continued.

with the vehicle treatment was observed when they were administered in combination.

Ox-LDL has been proposed as a more atherogenic lipoprotein particle than LDL-C (Steinberg, 1997), so we next examined whether monotherapies or the combination of these agents affect the plasma ox-LDL level. DS-9001a monotherapy reduced the plasma ox-LDL level compared with that on vehicle treatment, and ox-LDL was further reduced when atorvastatin and DS-9001a were administered in combination. In addition to non-HDL-C reduction, these results suggest that DS-9001a and atorvastatin have a synergistic effect on the reduction of plasma ox-LDL level.

Discussion

Anti-PCSK9 antibody therapy has been shown to induce a major reduction of plasma LDL-C level and has also recently been associated with a reduction of cardiovascular events in patients with atherosclerotic cardiovascular disease who were receiving statin therapy (Sabatine et al., 2017). Therefore, PCSK9 inhibition is thought to be an attractive therapy for hypercholesterolemia.

In the present study, we generated a novel small biologic alternative to PCSK9 antibodies, DS-9001a, which can be produced by using a bacterial expression system. DS-9001a inhibits the binding of PCSK9 to LDL-R in vitro; thus, DS-9001a attenuated PCSK9-mediated LDL-R degradation both in vitro and in vivo. We also observed that DS-9001a treatment enhanced LDL-C clearance and non-HDL-C reduction in mice. In addition, the sustained LDL-C lowering effect of DS-9001a was observed in cynomolgus monkeys. We also found an increase in hepatic LDL-R upon DS-9001a injection and observed a further LDL-R increase on combination treatment of atorvastatin and DS-9001a. In line with this, this combination exhibited a greater reduction in non-HDL-C level than the corresponding monotherapies. These findings are generally consistent with the properties of anti-PCSK9 antibodies. Therefore, we successfully produced a small biologic molecule that can be produced by a bacterial expression system, showing pharmacologic and

pharmacokinetic profiles comparable with those of therapeutic antibody.

In our study, the extent of non-HDL-C reduction for the combination of atorvastatin and DS-9001a was more pronounced than the combination of atorvastatin and anacetrapib. In clinical trials, anti-PCSK9 antibodies typically reduce the LDL-C level by approximately 60%, and anacetrapib reduces LDL-C by about 45% (Barter et al., 2015). Thus, the pharmacologic effect shown in our data were almost consistent with the clinical data. Here, anacetrapib treatment increased plasma HDL-C, whereas a reduction in plasma HDL-C was observed on combined treatment with DS-9001a and atorvastatin. The plasma HDL-C reduction shown in PCSK9 inhibition, however, is thought to be a specific phenomenon in rodents (Rashid et al., 2005; Mitchell et al., 2014). To investigate the precise impact of the lipid-modulating effects of these compounds to prevent cardiovascular events, further clinical study is required.

Increasing evidence has shown that ox-LDL is more atherogenic than native LDL-C (Steinberg, 1997), and the plasma ox-LDL level was significantly elevated in patients with coronary artery disease (Holvoet et al., 1998). In this study, DS-9001a–treated mice exhibited plasma ox-LDL reduction, whereas anacetrapib did not reduce ox-LDL. It is known that ox-LDL exists in various forms, characterized by different degrees of oxidation and different regions where oxidation has occurred (Parthasarathy et al., 2010). Here, we measured plasma ox-LDL by using the antibody 4E6, which was previously used to show the correlation between plasma ox-LDL and coronary artery disease (Holvoet et al., 1998). Therefore, besides the LDL-C–lowering effect, the ox-LDL reducing effect is a possible contributor to the reduction of cardiovascular events by PCSK9 inhibition therapy. Among the monotherapies, only DS-9001a monotherapy reduced the plasma ox-LDL level compared with that on vehicle administration, despite the similar reductions of non-HDL-C between atorvastatin and DS-9001a treatments. It is thought that statin treatment increases hepatic LDL-R level, which is the main mechanism behind its LDL-C–lowering effect in humans (Lennernäs and Fager, 1997). In contrast, in mice, statin is reported not to increase hepatic LDL-R levels and to reduce non-HDL-C mainly through inhibiting very-low-density lipoprotein cholesterol production (Rashid et al., 2005). Here, we also did not observe hepatic LDL-R elevation in statin-treated mice. In addition, ox-LDL was further reduced when atorvastatin and DS-9001a were administered in combination, the same condition in which a further increase in hepatic LDL-R levels was observed. These results suggest that ox-LDL reduction is correlated with the hepatic LDL-R level.

Given the high cost of anti-PCSK9 antibody therapy, which is about 100 times more expensive than statin treatment, discussions among health care providers, guideline committees, and payers are required to identify whom to treat with this therapy (Preiss and Baigent, 2017). The large patient population, together with the chronic state of the disease requiring lifelong treatment, indicates the benefits that less expensive PCSK9 inhibitors would have for both patients and the finances of health care systems. In this regard, microbial expression, by which DS-9001a can be produced, is considered suitable for large-scale production at lower costs. The small size of DS-9001a (a molecular weight of about 22 kDa) enables higher stoichiometric drug concentrations (4.5 mM) to be achieved compared with those for anti-PCSK9 antibodies [e.g., 140 mg/ml evolocumab (about 1.0 mM) and 150 mg/ml alirocumab (about 1.0 mM)]. Considering that two PCSK9 molecules can be captured by one anti-PCSK9 antibody, whereas DS-9001a reveals a 1:1 interaction, the higher achievable drug concentration of DS-9001a could lead to a smaller administration volume compared with those for antibody drugs. Moreover, the longer terminal $t_{1/2}$ of DS-9001a (128 ± 90 hours) than that of AMG145 (61 ± 9 hours) (Chan et al., 2009) in cynomolgus monkey correlates nicely with an extended pharmacologic effect, as observed on single intravenous administration of 3 mg/kg of the drug. This led to an LDL-C–lowering effect up to 21 days, but only for 14 days for the anti-PCSK9 antibody AMG145. Although we did not directly compare the durations of LDL-C reduction of DS-9001a and other anti-PCSK9 antibodies, the LDL-C–lowering effect of DS-9001a seems to last longer than that of other anti-PCSK9 antibodies (Liang et al., 2012; Zhang et al., 2012). In clinical studies, evolocumab, AMG145, is dosed at 420 mg/body every month or 140 mg/body every 2 weeks (Sabatine et al., 2017), and alirocumab is injected at 75 or 150 mg/body every 2 weeks (Schwartz et al., 2014). The dosing regimen of evolocumab (420 mg/body per month) requires three consecutive injections with a syringe containing 1 ml of drug each (https://www.accessdata.fda.gov/drugsatfda_docs/label/2015/125522s000lbl.pdf). It is reported that the dosing volume of subcutaneously administered drugs is closely related to their Visual Analogue Scale score (Jørgensen et al., 1996), an indicator of pain on injection. Therefore, the smaller administration volume for DS-9001a is a clear advantage as it avoids the burden of multiple high-volume injections. Additionally, the longer duration of LDL-C–lowering of DS-9001a may enable extension of the dose interval, which in turn reduces the frequency of injections and hospital visits. Since it was reported that drugs with a low price, low dosing frequency, and small dosing volume show high medication adherence in injection therapy (Tkacz et al., 2014), the characteristics of DS-9001a would be preferred as a PCSK9 inhibitor. The safety profile of Anticalin therapeutics is supported by positive phase 1 study results for Angiocal, another Anticalin protein targeting VEGF-A (Mross et al., 2013). For DS-9001a, we have not observed any treatment-related adverse effects on the single dosing of cynomolgus monkeys. Generally, this type of new biologic approach could be susceptible to the formation of antidrug antibodies. Although we used human tear lipocalin mutein to generate DS-9001a to reduce the risk of antidrug antibodies forming, we need to be vigilant on this issue in clinical study. Taking these findings together, although the safety profile and efficacy of DS-9001a in humans require further investigation, DS-9001a could become an attractive PCSK9 inhibitor.

Since Anticalin proteins are rapidly eliminated from the body owing to their small size (approximately 17 kDa), an ABD was fused to Anticalin protein's C-terminus to prolong its plasma $t_{1/2}$ by binding to HSA. Several other technologies that can extend the $t_{1/2}$ of drugs have been reported, such as site-directed PEGylation (Roberts et al., 2002), direct fusion of albumin (70 kDa) to drugs (Osborn et al., 2002), or fusion to the Fc portion of an antibody (Wu and Sun, 2014). The smaller size and structural simplicity of an Anticalin protein-ABD fusion facilitates the manufacturing process using a microbial expression system and confers a $t_{1/2}$ similar to those of antibodies. To the best of our knowledge, this is the first time that an ABD fusion protein has been shown to have a prolonged $t_{1/2}$

and sustained efficacy in nonhuman primates. Given the growing demand for antibody-like drugs, ABD-fused Anticalin proteins could represent a promising new class of small biologic molecules for wider therapeutic targets.

In conclusion, we created a novel small biologic alternative to PCSK9 antibodies, DS-9001a. DS-9001a potently binds to PCSK9, thereby preventing PCSK9-mediated LDL-R degradation. A reduction of LDL-C by approximately 62.4% was observed after single DS-9001a injection in cynomolgus monkeys, and this effect was sustained up to 3 weeks. Besides its robust pharmacology, DS-9001a can be manufactured by using a microbial expression system, possibly reducing production costs. Furthermore, the high solubility and smaller size of the ABD-fused Anticalin protein enable the administration of higher drug concentrations at lower volumes, which can improve patient compliance by reducing the burden of multiple painful injections. Therefore, DS-9001a may have potential as a new therapeutic option to treat patients with dyslipidemia. In addition, since the ABD-fused Anticalin protein reveals similar characteristics to antibodies in terms of target specificity and long pharmacokinetics, this novel technology could be applicable for a wider range of therapeutic areas in which antibodies are prescribed.

Acknowledgments

We thank Haruka Endo, Dr. Takanori Aoki, and Makoto Yoshida for their experimental assistance and Manabu Kato, Dr. Yoichiro Shiba, Dr. Koichi Nonaka, and Dr. Jun Hasegawa for helpful suggestions.

Authorship Contributions

Participated in research design: Masuda, Yamaguchi, Nara, Hashimoto, Nishizawa.

Conducted experiments: Masuda, Yamaguchi, Nagano, Miyauchi, E. Suzuki, Yamamura, Nishizawa.

Contributed new reagents and analytic tools: C. Suzuki, Aburatani, Nagatomo, Ishihara, Okuno, Hashimoto, Takahashi.

Performed data analysis: Masuda, Nagano, Miyauchi, E. Suzuki, Yamamura, Nishizawa.

Wrote or contributed to the writing of the manuscript: Masuda, Yamaguchi, Hashimoto, Matschiner, Nishizawa.

References

Abifadel M, Rabès JP, Devillers M, Munnich A, Erlich D, Junien C, Varret M, and Boileau C (2009) Mutations and polymorphisms in the proprotein convertase subtilisin kexin 9 (PCSK9) gene in cholesterol metabolism and disease. *Hum Mutat* **30**:520–529.

Barter PJ, Tabet F, and Rye KA (2015) Reduction in PCSK9 levels induced by anacetrapib: an off-target effect? *J Lipid Res* **56**:2045–2047.

Bochem AE, Kuivenhoven JA, and Stroes ES (2013) The promise of cholesteryl ester transfer protein (CETP) inhibition in the treatment of cardiovascular disease. *Curr Pharm Des* **19**:3143–3149.

Cameron J, Holla ØL, Ranheim T, Kulseth MA, Berge KE, and Leren TP (2006) Effect of mutations in the PCSK9 gene on the cell surface LDL receptors. *Hum Mol Genet* **15**:1551–1558.

Chan JC, Piper DE, Cao Q, Liu D, King C, Wang W, Tang J, Liu Q, Higbee J, Xia Z, et al. (2009) A proprotein convertase subtilisin/kexin type 9 neutralizing antibody reduces serum cholesterol in mice and nonhuman primates. *Proc Natl Acad Sci USA* **106**:9820–9825.

Dadu RT and Ballantyne CM (2014) Lipid lowering with PCSK9 inhibitors. *Nat Rev Cardiol* **11**:563–575.

Dubuc G, Chamberland A, Wassef H, Davignon J, Seidah NG, Bernier L, and Prat A (2004) Statins upregulate PCSK9, the gene encoding the proprotein convertase neural apoptosis-regulated convertase-1 implicated in familial hypercholesterolemia. *Arterioscler Thromb Vasc Biol* **24**:1454–1459.

Gille H, Hülsmeyer M, Trentmann S, Matschiner G, Christian HJ, Meyer T, Amirkhosravi A, Audoly LP, Hohlbaum AM, and Skerra A (2016) Functional characterization of a VEGF-A-targeting Anticalin, prototype of a novel therapeutic human protein class. *Angiogenesis* **19**:79–94.

Ginsberg HN (1998) Effects of statins on triglyceride metabolism. *Am J Cardiol* **81** (4A):32B–35B.

Holvoet P, Vanhaecke J, Janssens S, Van de Werf F, and Collen D (1998) Oxidized LDL and malondialdehyde-modified LDL in patients with acute coronary syndromes and stable coronary artery disease. *Circulation* **98**:1487–1494.

Jørgensen JT, Rømsing J, Rasmussen M, Møller-Sonnergaard J, Vang L, and Musaeus L (1996) Pain assessment of subcutaneous injections. *Ann Pharmacother* **30**:729–732.

Kim HJ, Eichinger A, and Skerra A (2009) High-affinity recognition of lanthanide(III) chelate complexes by a reprogrammed human lipocalin 2. *J Am Chem Soc* **131**:3565–3576.

Lennernäs H and Fager G (1997) Pharmacodynamics and pharmacokinetics of the HMG-CoA reductase inhibitors: similarities and differences. *Clin Pharmacokinet* **32**:403–425.

Liang H, Chaparro-Riggers J, Strop P, Geng T, Sutton JE, Tsai D, Bai L, Abdiche Y, Dilley J, Yu J, et al. (2012) Proprotein convertase substilisin/kexin type 9 antagonism reduces low-density lipoprotein cholesterol in statin-treated hypercholesterolemic nonhuman primates. *J Pharmacol Exp Ther* **340**:228–236.

Malyala P and Singh M (2008) Endotoxin limits in formulations for preclinical research. *J Pharm Sci* **97**:2041–2044.

Matschiner G, Rothe C, Hohlbaum A, Siham Bel AR, Hinner M, Allersdorfer A, Lunde B, Wiedenmann A, Yamaguchi S, Aburatani T, et al. (2014) inventors, Daiichi Sankyo Co Ltd, assignee. Novel binding proteins for PCSK9. WO 2014/140210 A1. 2014 Sept 18.

Millar JS, Reyes-Soffer G, Jumes P, Dunbar RL, deGoma EM, Baer AL, Karmally W, Donovan DS, Rafeek H, Pollan L, et al. (2015) Anacetrapib lowers LDL by increasing ApoB clearance in mildly hypercholesterolemic subjects. *J Clin Invest* **125**:2510–2522.

Mitchell T, Chao G, Sitkoff D, Lo F, Monshizadegan H, Meyers D, Low S, Russo K, DiBella R, Denhez F, et al. (2014) Pharmacologic profile of the Adnectin BMS-962476, a small protein biologic alternative to PCSK9 antibodies for low-density lipoprotein lowering. *J Pharmacol Exp Ther* **350**:412–424.

Mross K, Richly H, Fischer R, Scharr D, Büchert M, Stern A, Gille H, Audoly LP, and Scheulen ME (2013) First-in-human phase I study of PRS-050 (Angiocal), an Anticalin targeting and antagonizing VEGF-A, in patients with advanced solid tumors. *PLoS One* **8**:e83232.

Olwill SA, Joffroy C, Gille H, Vigna E, Matschiner G, Allersdorfer A, Lunde BM, Jaworski J, Burrows JF, Chiriaco C, et al. (2013) A highly potent and specific MET therapeutic protein antagonist with both ligand-dependent and ligand-independent activity. *Mol Cancer Ther* **12**:2459–2471.

Osborn BL, Olsen HS, Nardelli B, Murray JH, Zhou JX, Garcia A, Moody G, Zaritskaya LS, and Sung C (2002) Pharmacokinetic and pharmacodynamic studies of a human serum albumin-interferon-alpha fusion protein in cynomolgus monkeys. *J Pharmacol Exp Ther* **303**:540–548.

Parthasarathy S, Raghavamenon A, Garelnabi MO, and Santanam N (2010) Oxidized low-density lipoprotein. *Methods Mol Biol* **610**:403–417.

Preiss D and Baigent C (2017) Cardiovascular disease: PCSK9 inhibition: a new player in cholesterol-lowering therapies? *Nat Rev Nephrol* **13**:450–451.

Rashid S, Curtis DE, Garuti R, Anderson NN, Bashmakov Y, Ho YK, Hammer RE, Moon YA, and Horton JD (2005) Decreased plasma cholesterol and hypersensitivity to statins in mice lacking Pcsk9. *Proc Natl Acad Sci USA* **102**:5374–5379.

Roberts MJ, Bentley MD, and Harris JM (2002) Chemistry for peptide and protein PEGylation. *Adv Drug Deliv Rev* **54**:459–476.

Roddy TP, McLaren DG, Chen Y, Xie D, Dunn K, Kulick A, Szeto D, Forrest G, Albanese K, Donnelly M, et al. (2014) Effects of anacetrapib on plasma lipids, apolipoproteins and PCSK9 in healthy, lean rhesus macaques. *Eur J Pharmacol* **740**:410–416.

Sabatine MS, Giugliano RP, Keech AC, Honarpour N, Wiviott SD, Murphy SA, Kuder JF, Wang H, Liu T, Wasserman SM, et al.; FOURIER Steering Committee and Investigators (2017) Evolocumab and clinical outcomes in patients with cardiovascular disease. *N Engl J Med* **376**:1713–1722.

Schwartz GG, Bessac L, Berdan LG, Bhatt DL, Bittner V, Diaz R, Goodman SG, Hanotin C, Harrington RA, Jukema JW, et al. (2014) Effect of alirocumab, a monoclonal antibody to PCSK9, on long-term cardiovascular outcomes following acute coronary syndromes: rationale and design of the ODYSSEY outcomes trial. *Am Heart J* **168**:682–689.

Shimizugawa T, Ono M, Shimamura M, Yoshida K, Ando Y, Koishi R, Ueda K, Inaba T, Minekura H, Kohama T, et al. (2002) ANGPTL3 decreases very low density lipoprotein triglyceride clearance by inhibition of lipoprotein lipase. *J Biol Chem* **277**:33742–33748.

Skerra A (2008) Alternative binding proteins: anticalins - harnessing the structural plasticity of the lipocalin ligand pocket to engineer novel binding activities. *FEBS J* **275**:2677–2683.

Steinberg D (1997) Low density lipoprotein oxidation and its pathobiological significance. *J Biol Chem* **272**:20963–20966.

Tkacz J, Ellis L, Bolge SC, Meyer R, Brady BL, and Ruetsch C (2014) Utilization and adherence patterns of subcutaneously administered anti-tumor necrosis factor treatment among rheumatoid arthritis patients. *Clin Ther* **36**:737–747.

van der Tuin SJ, Kühnast S, Berbée JF, Verschuren L, Pieterman EJ, Havekes LM, van der Hoorn JW, Rensen PC, Jukema JW, Princen HM, et al. (2015) Anacetrapib reduces (V)LDL cholesterol by inhibition of CETP activity and reduction of plasma PCSK9. *J Lipid Res* **56**:2085–2093.

Wu B and Sun YN (2014) Pharmacokinetics of peptide-Fc fusion proteins. *J Pharm Sci* **103**:53–64.

Zhang L, McCabe T, Condra JH, Ni YG, Peterson LB, Wang W, Strack AM, Wang F, Pandit S, Hammond H, et al. (2012) An anti-PCSK9 antibody reduces LDL-cholesterol on top of a statin and suppresses hepatocyte SREBP-regulated genes. *Int J Biol Sci* **8**:310–327.

Zurdo J, Arnell A, Obrezanova O, Smith N, Gómez de la Cuesta R, Gallagher TR, Michael R, Stallwood Y, Ekblad C, Abrahmsén L, et al. (2015) Early implementation of QbD in biopharmaceutical development: a practical example. *BioMed Res Int* **2015**:605427.

Address correspondence to: Tomohiro Nishizawa, End-Organ Disease Laboratories, Daiichi Sankyo Co., Ltd., 1-2-58, Hiromachi, Shinagawa-ku, Tokyo 140-8710, Japan. E-mail: nishizawa.tomohiro.yk@daiichisankyo.co.jp

Generation and Characterization of a Novel Small Biologic Alternative to PCSK9 Antibodies, DS-9001a, Albumin Binding Domain-Fused Anticalin Protein

Authors
Yusuke Masuda†, Shinji Yamaguchi†, Chikako Suzuki, Takahide Aburatani, Yuki Nagano, Ryuki Miyauchi, Eiko Suzuki, Naotoshi Yamamura, Kentaro Nagatomo, Hidetoshi Ishihara, Kazuaki Okuno, Futoshi Nara, Gabriele Matschiner, Ryuji Hashimoto, Tohru Takahashi, and Tomohiro Nishizawa
†These two authors contributed equally to this work.

End-Organ Disease Laboratories, Daiichi Sankyo Co., Ltd., Tokyo, Japan (Y.M., Y.N., T.N.)
Venture Science Laboratories, Daiichi Sankyo Co., Ltd., Tokyo, Japan (S.Y.)
Modality Research Laboratories, Daiichi Sankyo Co., Ltd., Tokyo, Japan (C.S., T.A., R.M., R.H., T.T.)
Drug Metabolism & Pharmacokinetics Research Laboratories (E.S., N.Y.)
Biologics Technology Research Laboratories (K.O.)
Biologics & Immuno-Oncology Laboratories (F.N.)
Pieris Pharmaceuticals GmbH, Freising, Germany (G.M.)

Corresponding author
Tomohiro Nishizawa
1-2-58, Hiromachi, Shinagawa-ku, Tokyo 140-8710, Japan
Tel.: +81-3-3492-3131, Fax: +81-3-5436-8587
Email: nishizawa.tomohiro.yk@daiichisankyo.co.jp

Supplementary Method

Phagemid selection of optimized Anticalin proteins against PCSK9

For the selection of optimized PCSK9-specific Anticalin proteins, 2×10^{12} phagemids from the biased maturated libraries were used. Phagemids were dissolved in PBS supplemented with 0.1% Tween-20 (v/v) (PBS-0.1%T) containing 50 mM benzamidine and 1% (w/v) casein. To select Anticalin proteins with increased affinity, phagemids were incubated with reduced concentrations of biotinylated PCSK9 proteins that ranged from 0.01 to 10 nM. In several instances, phagemids were incubated at 65° C for 10 min to select for muteins with increased heat tolerance. Dissolved phagemids were incubated for 40 min with biotinylated PCSK9 proteins before 0.3 mM desthiobiotin was added to the solution to saturate free streptavidin binding sites and incubation was continued for 20 min. Subsequently, blocked [1% (w/v) casein in PBS-0.1%T] and drained paramagnetic beads that were coated with either streptavidin or neutravidin were added for 20 min to capture PCSK9-phagemid complexes. Uncomplexed phagemids were removed by washing the beads eight times with 1 mL of PBS-0.1%T by thorough resuspension followed by the collection of beads with a magnet. Bound phagemids were first eluted with 300 µL of 70 mM triethylamine for 10 min, followed by immediate neutralization of the supernatant with 100 µL of 1 M Tris-HCl pH 6.0. After one intermediate wash cycle, remaining phagemids were eluted with 100 mM glycine pH 2.2 for 10 min, followed by immediate neutralization with 50 µL of 0.5 M Tris-base. Both elution fractions were pooled and used to infect 4 mL of log-phase *E. coli* culture (OD_{550} 0.45–0.6) for reamplification. After incubation for 30 min under agitation, bacteria were collected by centrifugation at 5000 × g for 2 min, resuspended in 1 mL of 2xYT medium, and plated on three large LB/Amp agar plates (10 g/L bacto tryptone, 5 g/L yeast extract, 5 g/L NaCl, pH 7.5, 15 g/L agar, 100 µg/mL ampicillin). Plates were incubated overnight at 32° C. Infected cells were scraped from the agar plates using 50 mL of 2xYT medium supplemented with 100 µg/mL ampicillin (2xYT/Amp). A total of 50 mL of 2xYT/Amp medium was inoculated with the appropriate volume of bacterial suspension to reach an OD_{550} of 0.08. The culture was incubated at 37° C on a shaker (160 rpm) until an OD_{550} of 0.5 was reached and then infected with helper phages (1.5×10^{11} pfu) by incubation for 15 min with gentle agitation and for 45 min on a shaker at 37° C. Subsequently, kanamycin was added to a final concentration of 70 µg/mL to select for bacteria that had been infected by the helper phages. Finally, expression of the pIII-Anticalin proteins was induced by the addition of 25 ng/mL anhydrotetracycline. PCSK9-specific Anticalin proteins were selected by repeating the above cycle four times. For the specific selection of Anticalin proteins with reduced k_{off} rates, either a more stringent wash protocol was applied by performing 5 additional wash steps after round 1, 10 after round 2, 15 after round 3, and 20 after round 4 or Anticalin protein-PCSK9 complexes were incubated with different amounts (10 nM–5 µM) of purified parental Anticalin protein to allow competition in PCSK9 binding between optimized and parental Anticalin proteins. Additionally, combinations of both methods were applied.

Evaluation of DS-9001a pharmacokinetic profile in rat

DS-9001a or DS-9001a without ABD was intravenously injected into male SD rats (9 weeks old) at 10 or 7.6 mg/kg, respectively, which are equivalent to 0.45 μmol/kg (n=3). Administration was conducted at 2.0 mL/kg. Blood was collected from the tail vein at 0.5, 1, 2, 4, 6, 8, 10, 24, 48, and 72 h after injection. Plasma was obtained by centrifugation (12,000 rpm, 5 min, 4˚ C).

Ninety-six-well plates were coated with 25 μL/well of anti-protein 4 IgG, which binds to the Anticalin protein portion of DS-9001a (generated at Immuno-Biological Laboratories Co., Ltd., Fujioka, Japan), diluted to 2 μg/mL with PBS and incubated at 4˚ C for overnight. The plates were washed three times with 0.05% (v/v) Tween 20 in PBS (PBS-0.05%T) and blocked with 150 μL/well of PBS containing 3% (w/v) BSA for 1–2 h at room temperature. Standards were prepared using PBS-0.05%T containing 20% (v/v) rat plasma and 1% (w/v) BSA (20% rat plasma). Plasma samples were diluted fivefold with PBS-0.05%T containing 1% (w/v) BSA and then further diluted with 20% rat plasma, if necessary. After washing in the same manner as described above, 25 μL/well of the standard and diluted sample were added to the plates and incubated for 1–2 h at room temperature. Detection reagent was prepared by mixing the biotinylated anti-protein 4 IgG and Streptavidin Sulfo-Tag (Meso Scale Diagnostics, LLC, Rockville, MD) to make a concentration of 1 μg/mL each in PBS-0.05%T containing 1% (w/v) BSA; then, the mixture was left on ice for 1 h. After washing, 25 μL/well of the detection reagent was added to the plates and incubated for 1–2 h at room temperature. After the final washing step, 150 μL/well of 2x Read Buffer prepared by dilution of 4x MSD Read Buffer T with surfactant (Meso Scale Diagnostics, LLC) was added to the plates. Luminescence intensity was measured using SECTOR Imager (SI2400; Meso Scale Diagnostics, LLC). The standard curve ranges of DS-9001a and DS-9001a without ABD were 0.685–500 and 0.685–167 ng/mL, respectively. Standard regression was established using a four-parameter logistic curve fit with 1/y2 weighting in the Discovery Workbench 3.0 (Meso Scale Diagnostics, LLC). The measured concentration of DS-9001a or DS-9001a without ABD in each sample was automatically calculated by the software using the calibration curve and then converted to the plasma concentration by multiplying by the dilution factor using Microsoft Office Excel 2010 (Microsoft Corporation, Redmond, WA).

Pharmacokinetic parameters of DS-9001a and DS-9001a without ABD after administration to rats were calculated using Phoenix WinNonlin (version 6.3; Certara L.P., Princeton, NJ) based on a non-compartmental method. Calculation of the elimination rate constant for DS-9001a was automatically processed by the software. The elimination rate constant for DS-9001a without ABD was calculated using the slope of the regression line of 0.5 to 6 h after dosing.

Measurement of binding affinity of DS-9001a and DS-9001a without ABD to human PCSK9 and human serum albumin (HSA)

An HBS-EP+ buffer (10 mM HEPES, pH 7.4, 0.15 M NaCl, 3 mM EDTA, and 0.05% surfactant P20) was used as running buffer. A Biotin CAPture kit (GE Healthcare) was used to immobilize the biotinylated PCSK9 ligand to sensor chips. For capture experiments, streptavidin-DNA conjugates were injected to two flowcells for 20 s, and the biotinylated PCSK9 samples were diluted to 1 ng/µL in the running buffer and then injected to one flowcell for 1 min at 10 µL/min, whereas another flowcell was left without captured samples to provide a reference surface. The capture protocol was designed to yield capture levels of ligand samples that resulted in R_{max} values no greater than 20 RU.

For each kinetic experiment, varying concentrations of purified DS-9001a and DS-9001a without ABD ranging from 0.03 to 100 nM were prepared as the analytes, and injected for 300 s at 30 µL/min followed by 30 min of dissociation. Captured and reference surfaces were regenerated with a 2-min pulse of 6 M guanidine hydrochloride in 0.25 M sodium hydroxide. The binding affinity of DS-9001a to HSA was also measured in the same assay.

The association rate constants (k_a), dissociation rate constants (k_d), and the resulting dissociation constants (K_D) were calculated using a 1:1 Langmuir binding model. The raw data sets were analyzed using Biacore T200 Evaluation Software (version 1.0; GE Healthcare), and the sensorgrams of the reference flowcells were subtracted from the sensorgrams of the sample-captured flowcells.

Plasma DS-9001a concentrations in cynomolgus monkeys

Plasma DS-9001a concentrations were determined by sandwich ELISA, using anti-DS-9001a antibody (Daiichi Sankyo Co., Ltd.) and biotinylated anti-DS-9001a antibody (Shin Nippon Biomedical Laboratories, Ltd.).

Supplementary Figures

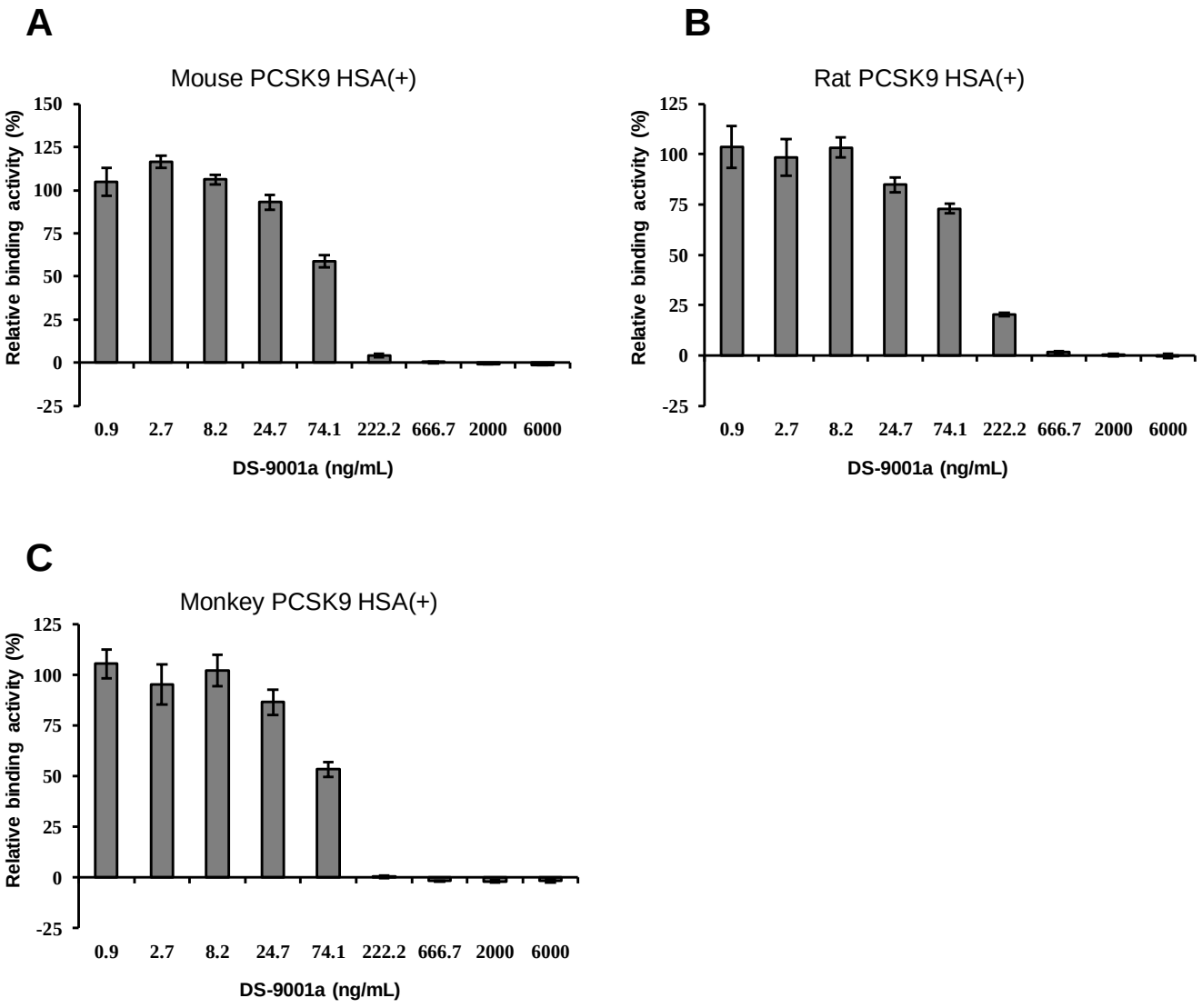

Supplementary Figure 1

DS-9001a inhibits degradation of LDL-R induced by mouse, rat, and monkey PCSK9

(A–C) Biotin-labeled mouse, rat, and monkey PCSK9 and DS-9001a were added to an anti-LDL-R antibody-coated plate in the presence of human serum albumin (HSA). Then, human LDL-R was added to the plate and the plate was incubated for 2 h. The level of PCSK9 captured by LDL-R was detected with streptavidin-HRP. As positive and negative controls, DS-9001a-deficient and LDL-R-deficient wells were prepared, respectively. The relative binding activity (%) was calculated using the following equation: Relative binding activity = [(luminescent signal in each well) – (luminescent signal in negative control wells)] / [(luminescent signal in positive control wells) − (luminescent signal in negative control wells)] × 100. The results are presented as mean ± SE (n=3).

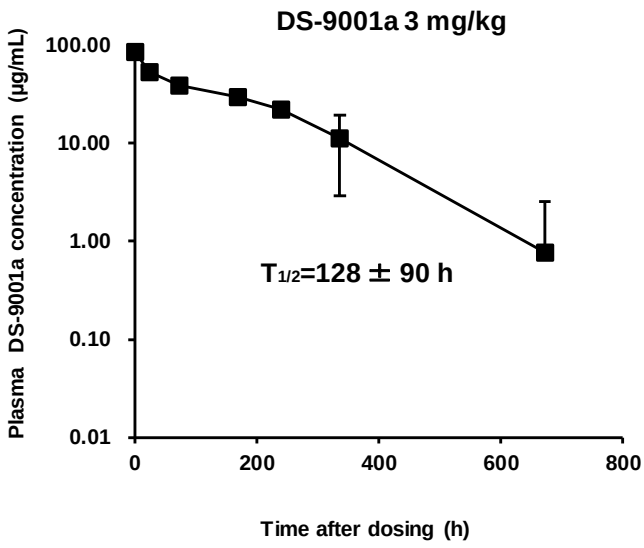

Supplementary Figure 2

Plasma DS-9001a concentrations after single DS-9001a injection into cynomolgus monkeys

DS-9001a at 3 mg/kg was intravenously administered to cynomolgus monkeys and the blood was collected at specific time points. Plasma total DS-9001a level was measured. The data are presented as mean ± SD (n=6).